

Electronic Supplementary Information for

A photoluminescent dinuclear phenylquinolyl Ir(II)-Ir(II) complex featuring a $\mu\text{-}\eta^1\text{:}\eta^2$ -phenylquinolyl bridge and an end-on dinitrogen ligand†

Wei Yang, Songlin Zhang^{*}, Yuqiang Ding^{*}, Li Shi and Qijun Song

Received (in XXX, XXX) Xth XXXXXXXXX 200X, Accepted Xth XXXXXXXXX 200X

First published on the web Xth XXXXXXXXX 200X

DOI: 10.1039/b000000x

Contents:

- (1) Experimental details and physical data
- (2) X-ray crystallography
- (3) Computational Method
- (4) S-reference
- (5) Figure S1, Figure S2, Figure S3, Figure S4, Figure S5, Figure S6 and Figure S7

Figure S1. ORTEP diagram of complex **2** with thermal ellipsoids shown at the 30% probability level.

Figure S2. UV-vis absorption and normalized PL emission spectra of complex **2**

Figure S3. Absorption spectrum of complex **2** in 400-700 nm range

Figure S4. UV-vis absorption spectra of complex **2** and pq

Figure S5. IR spectrum of complex **2**

Figure S6. IR spectrum of reactant admixture after reaction of complex **2** with triphenylphosphine

Figure S7. IR spectrum of complex **2** after excitation and photoluminescence

(6) Table S1, Table S2 and Table S3

Table S1. Selected Geometric Parameter by X-Ray Single Crystal Diffraction and Calculations B3LYP/6-31G* Levels for Complex **2**

Table S2. Calculated Absorption of Complex **2** in CH₂Cl₂ Media at TD-B3LYP Level, Together with Experimental Values

Table S3. The photophysical properties of complex **2**

Table S4. The UV-vis absorption wavelength of complex **2** and pq

(1) Experimental details and physical data

All the synthetic procedures involving iridium species and sodium methanolate were carried out in dry argon or nitrogen atmosphere by using a standard Schlenk tube, the main concern is on the oxidative stability of intermediate complexes and moisture-sensitive sodium methanolate used in the reaction.

Materials. IrCl₃·3H₂O and other chemicals were obtained from commercial resource and used without further purification. 2-phenylquinoline (pq)^[S1] and Chloro-bridged dimer (pq)₂Ir(μ-Cl)₂Ir(pq)₂^[S2] were synthesized according to the reported papers. All Solvents were dried by standard methods.

Characterization methods. IR spectra were recorded on a FTLA2000 spectrometer by dispersing samples in potassium bromide. NMR spectra were collected on a Bruker ACF-400 spectrometer with CD₂Cl₂ as solvent and tetramethylsilane as

internal standard. Absorption spectra were measured using a UV/Vis spectrophotometer (Model TU-1901). PL spectra were obtained using RF-5301PC spectrofluorimeter (Shimadzu, Japan) connected to a photomultiplier tube with a Xenon lamp as the excitation source. The PL quantum yields were measured in degassed dichloromethane solutions, using tris(8-hydroxyquinoline) aluminum (Alq3) in DMF ($\Phi_{\text{PL}}=0.116$)^[S3] as a reference. A mass spectrum was obtained by Mass Spectrometry (Waters Maldi Synapt Q-TOF, USA) with positive ESI mode. Elemental analysis was performed on a Vrioel III analyzer (Elementar, Germany).

Synthesis of Complex 2. [(pq)₂IrCl]₂ (0.512 g, 0.40 mmol) and sodium methanolate (0.256g, 4.74mmol) was placed in a Schlenk tube containing 20 mL of ethoxyethanol. The mixture was stirred at 110°C for 20 h, resulting in a deep dark red suspension. The suspension was poured into 40 mL of pure water, and the precipitate was filtered off, washed with deionized water (10ml×5) and n-hexane (10ml×5), and then followed by drying at 60°C in a vacuum oven. The crude product was dissolved again in dichloromethane (20 mL) and adsorbed on silica gel and rapidly further purified by column chromatography over silica gel using n-hexane-CH₂Cl₂ (3/1-3/2) as eluent to obtain complexes **2** in 22% yield (0.090 g). The dark red crystal obtained was recrystallized from a dichloromethane/hexane mixture. IR (KBr): 3043 w, 2014 vs, 1833 w, 1603 1578 s, 1545 w, 1513 s, 1442 w, 1335 m, 1289 1148 1086 1046 w, 829 m, 789 w, 762 s, 731 w. ¹H NMR (δ , CD₂Cl₂): 9.73 (m, 1H), 9.39 (d, J = 8.2 Hz, 1H), 8.34-8.24 (m, 3H), 8.16-8.13 (m, 2H), 7.98 (dd, J = 8.8 Hz, 14.8 Hz, 2H), 7.93 (d, J = 1.2 Hz, 1H), 7.86-7.81 (m, 2H), 7.77-7.69 (m, 3H), 7.59-7.52 (m,

2H), 7.34 (d, $J = 2.0$ Hz, 1H), 7.22-7.18 (m, 2H), 6.99 (m, 2H), 6.91 (m, 1H), 6.80-6.68 (m, 4H), 6.28 (m, 1H), 6.14 (m, 1H). ^{13}C NMR (δ , CD_2Cl_2): 172.52, 168.87, 166.73, 166.62, 157.13, 153.68, 147.80, 147.14, 145.49, 145.34, 145.00, 143.71, 141.23, 138.27, 137.17, 136.86, 136.80, 131.66, 130.63, 130.45, 129.86, 129.62, 129.45, 129.23, 129.15, 129.13, 127.51, 127.45, 127.22, 126.59, 126.25, 126.09, 125.83, 125.81, 125.76, 124.66, 123.97, 122.77, 121.92, 120.92, 119.76, 117.66, 116.42, 114.84. Anal. Found for $\text{C}_{45}\text{H}_{29}\text{Ir}_2\text{N}_5$: C, 52.71; H, 2.69; N, 6.78; Cald. C, 52.77; H, 2.85; N, 6.84. MS (ESI⁺, m/z): 1025 [M+H].

(2) X-ray crystallography:

X-Ray data for compound **2** were collected using a Bruker SMART APEX II CCD area detector using monochromated Mo-K α radiation ($\lambda = 0.71073$ Å). The crystal of **2** was measured at 293(2) K. The structure was solved by direct phase determination (SHELXS-97) and refined for all data by full-matrix least squares methods on F^2 . All non-hydrogen atoms were subjected to anisotropic refinement and were generated geometrically and allowed to ride on their respective parent atoms. X-ray structural information (CIF) for complex **2** is available free of charge via the Internet at <http://www.rcs.org>.

(3) Computational Method

Calculations on the electronic ground state of complex **2** were performed using B3LYP density functional theory.^[S4] A 6-31G(d) basis set was implemented for the first-, and second-row elements H, C and N, whereas the LANL2DZ basis set was

employed for Ir. The ground-state B3LYP calculations were carried out using the Gaussian 03 suite of programs.^[S5] The calculated structural parameters (in table 1) are in good agreement with the crystallographic data. On the basis of the optimized ground-state, the absorption property in dichloromethane (CH₂Cl₂) media was calculated by time-dependent DFT (TDDFT)^[S6] associated with the polarized continuum model (PCM).^[S7]

(4) S-reference:

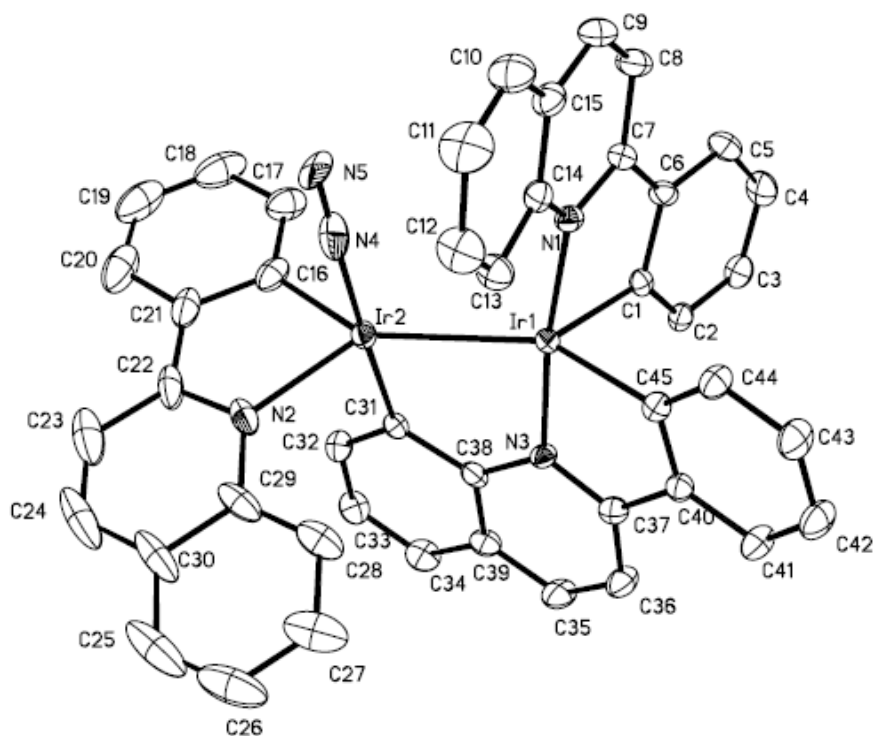
- [S1] A. Li, E. Ahmed, X. Chen, M. Cox, A. Crew, H. Dong , M. Jin, L. Ma, B. Panicker, K. Siu, A. Steinig, K. Stolz , P. Tavares, B. Volk, Q. Weng, D. Werner and M. Mulvihill, *J. Org. Biomol. Chem.*, 2007, **5**, 61.
- [S2] (a) M. Nonoyama, *Bull. Chem. Soc. Jpn.*, 1974, **47**, 767. (b) S. Sprouse, K. A. King, P. J. Spellane and R. J. Watts, *J. Am. Chem. Soc.*, 1984, **106**, 6647. (c) F. O. Garces, K. A. King and R. J. Watts, *Inorg. Chem.*, 1988, **27**, 3464.
- [S3] F. E. Lytle, D. R. Story and M. E. Juricich, *Spectrochim. Acta, Part A*, 1973, **29**, 1357.
- [S4] (a) C. Lee, W. Yang and R. G. Parr, *Phys. Rev. B*, 1988, **37**, 785; (b) A. D. Becke, *J. Chem. Phys.*, 1993, **98**, 5648.
- [S5] M. J. Frisch, G. W. Trucks, H. B. Schlegel, G. E. Scuseria, M. A. Robb, J. R. Cheeseman, J. A. J. Montgomery, T. Vreven, K. N. Kudin, J. C. Burant, J. M. Millam, S. S. Iyengar, J. Tomasi, V. Barone, B. Mennucci, M. Cossi, G. Scalmani,

N. Rega, G. A. Petersson, H. Nakatsuji, M. Hada, M. Ehara, K. Toyota, R. Fukuda, J. Hasegawa, M. Ishida, T. Nakajima, Y. Honda, O. Kitao, H. Nakai, M. Klene, X. Li, J. E. Knox, H. P. Hratchian, J. B. Cross, V. Bakken, C. Adamo, J. Jaramillo, R. Gomperts, R. E. Stratmann, O. Yazyev, A. J. Austin, R. Cammi, C. Pomelli, J. W. Ochterski, P. Y. Ayala, K. Morokuma, G. A. Voth, P. Salvador, J. J. Dannenberg, V. G. Zakrzewski, S. Dapprich, A. D. Daniels, M. C. Strain, O. Farkas, D. K. Malick, A. D. Rabuck, K. Raghavachari, J. B. Foresman, J. V. Ortiz, Q. Cui, A. G. Baboul, S. Clifford, J. Cioslowski, B. B. Stefanov, G. Liu, A. Liashenko, P. Piskorz, I. Komaromi, R. L. Martin, D. J. Fox, T. Keith, M. A. Al-Laham, C. Y. Peng, A. Nanayakkara, M. Challacombe, P. M. W. Gill, B. Johnson, W. Chen, M. W. Wong, C. Gonzalez and J. A. Pople, *Gaussian 03, Revision E.01*; Gaussian, Inc.: Wallingford, CT, 2004.

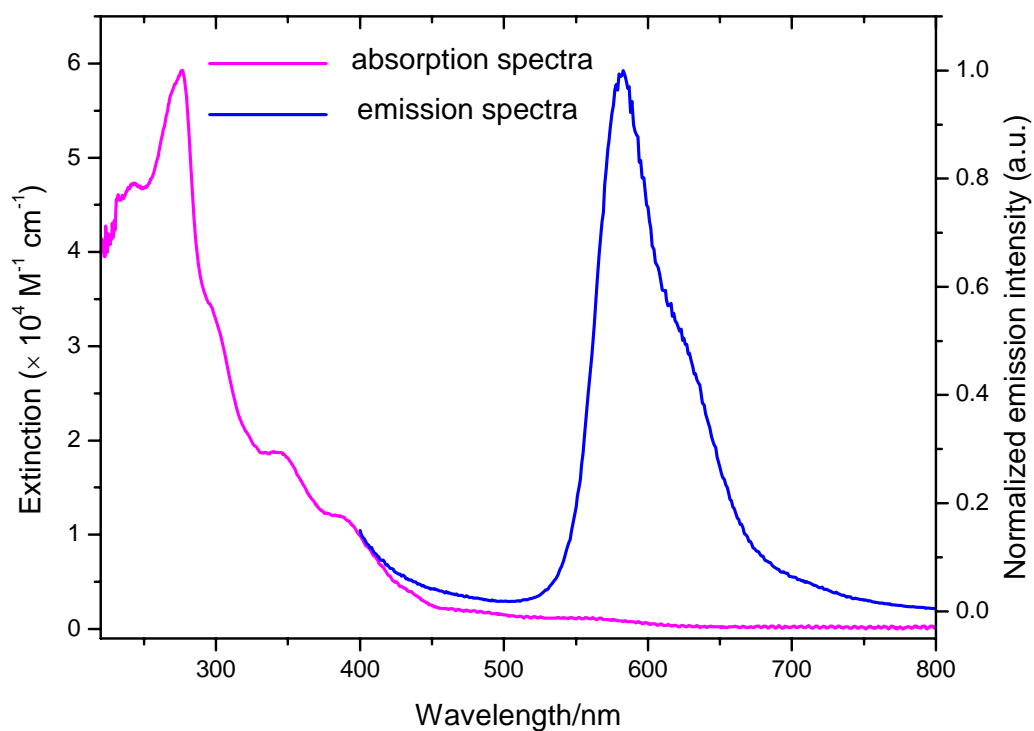
[S6] (a) M. E. Casida, C. Jamorski, K. C. Casida and D. R. Salahub, *J. Chem. Phys.* 1998, **108**, 4439; (b) R. E. Stratmann, G. E. Scuseria, and M. J. Frisch, *J. Chem. Phys.*, 1998, **109**, 8218; (c) N. N. Matsuzawa, A. Ishitani, D. A. Dixon and T. Uda, *J. Phys. Chem. A.*, 2001, **105**, 4953.

[S7] (a) V. Barone, M. Cossi, and J. Tomasi, *J. Chem. Phys.*, 1997, **107**, 3210; (b) M. Cossi, G. Scalmani, N. Rega, and V. Barone, *J. Chem. Phys.*, 2002, **117**, 43.

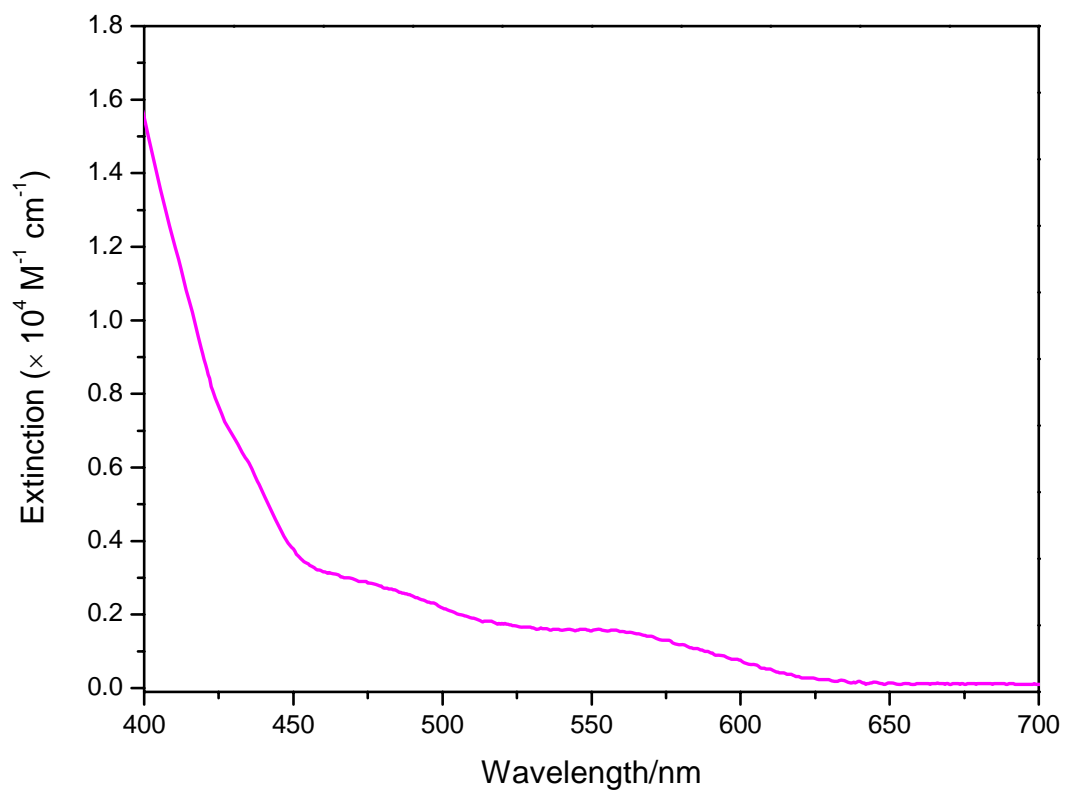
(5) **Figure S1.** ORTEP diagram of complex **2** with thermal ellipsoids shown at the 30% probability level. The hydrogen atoms have been omitted for clarity.



(5) Figure S2. UV-vis absorption and normalized PL emission spectra of complex **2** recorded in CH₂Cl₂ solution with a concentration of 10⁻⁵ mol/L. Luminescence measurements were carried out at $\lambda_{\text{ex}} = 360$ nm.

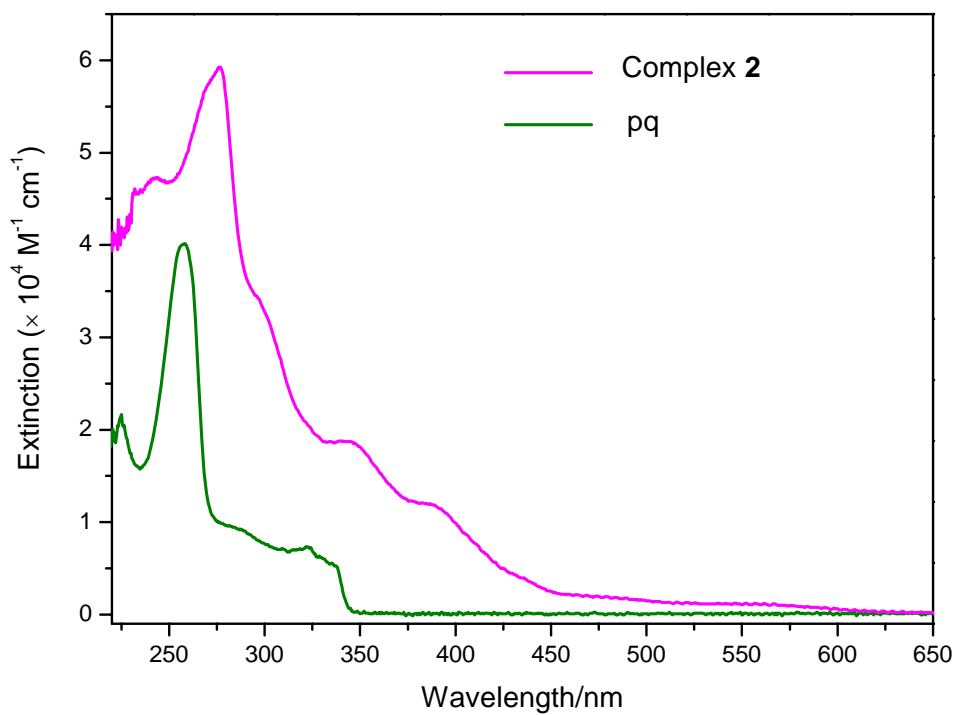


(5) Figure S3. The absorption spectrum of complex **2** (400-700nm range) in CH₂Cl₂ solution with a concentration of 5×10^{-5} mol/L.

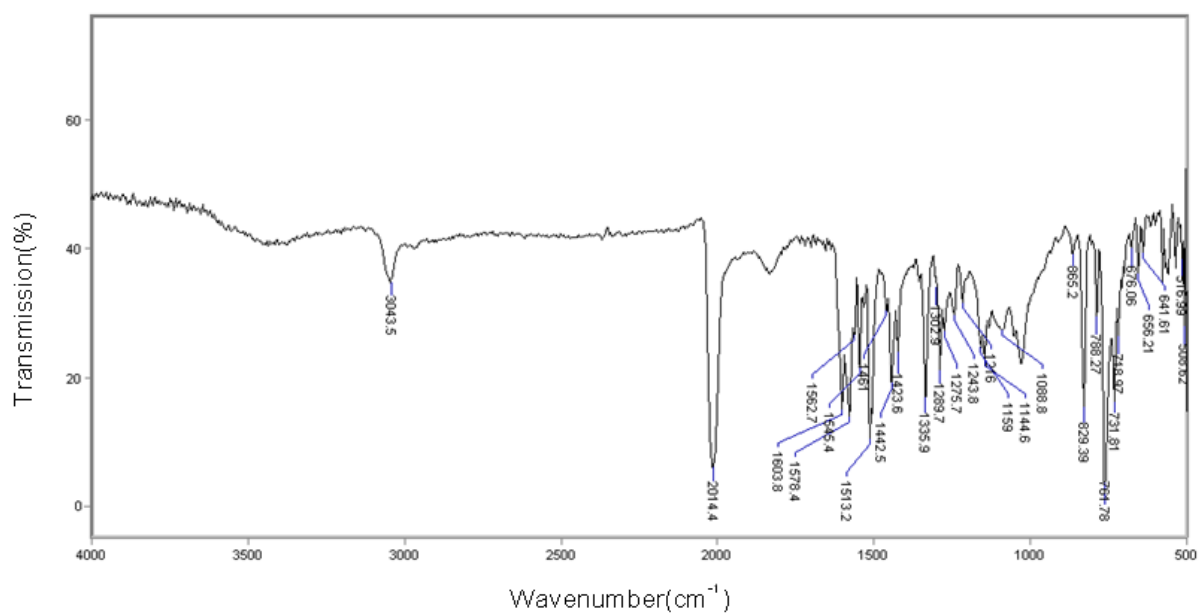


(5) Figure S4. UV-vis absorption spectra of complex **2** and free phenylquinoline (pq)

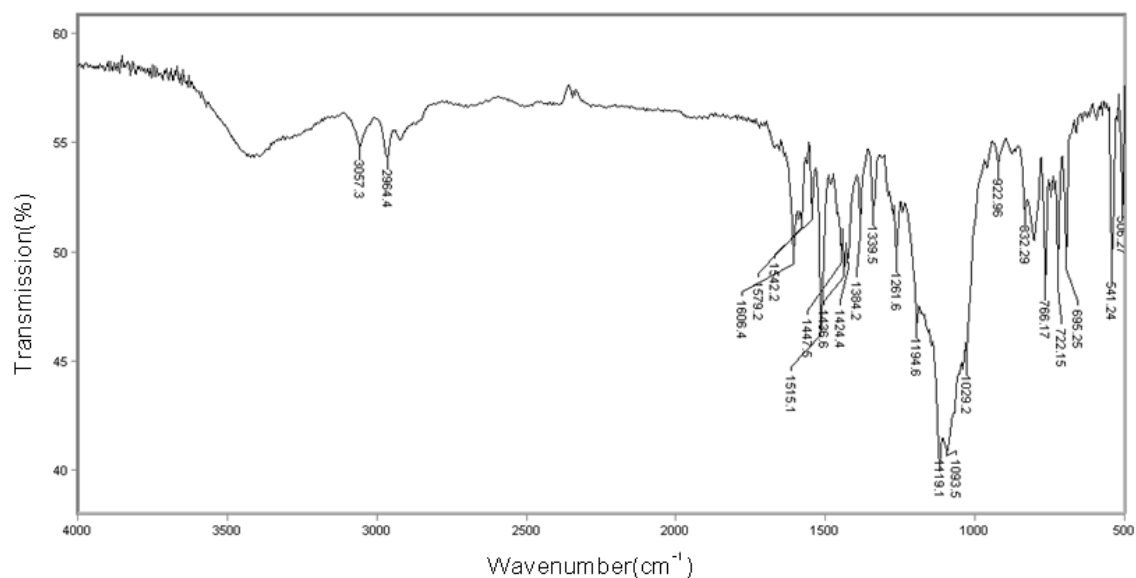
in CH₂Cl₂ solution with a concentration of 10⁻⁵ mol/L.



(5) Figure S5. IR spectrum of complex 2

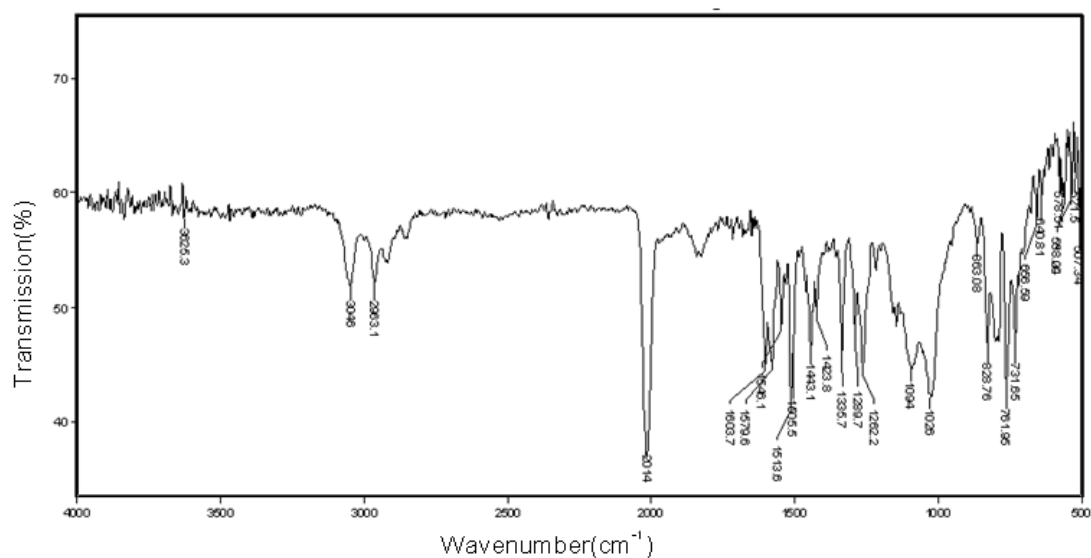


(5) **Figure S6.** IR spectrum of product mixture from reaction of complex **2** with triphenylphosphine.



Complex **2** (0.058 g, 0.057 mmol) and triphenylphosphine (0.022 g, 0.084 mmol) was placed in a Schlenk tube containing 10 mL of CH₂Cl₂. The mixture was stirred and refluxed for 6 h. The volatiles of the product mixture were then removed under vacuum and the IR spectrum of the residue was recorded as shown by Figure S6. The characteristic absorption band at 2014 cm⁻¹ disappears, which indicates that dinitrogen ligand is lost after reaction of complex **2** with triphenylphosphine, possibly due to substitution by triphenylphosphine ligand.

(5) **Figure S7.** IR spectrum of complex **2** after excitation and photoluminescence



To unambiguously demonstrate that dinitrogen ligand remains bound to Ir center during irradiation and photoluminescence process, after excitation and photoluminescence experiment for complex **2**, the solution was dried and the resulting powder was subjected to IR spectroscopy study. As shown by Figure S7, the characteristic intense absorption band at 2014 cm^{-1} remains, demonstrating that dinitrogen ligand still remains bound to Ir center.

(6) Table S1. Selected Geometric Parameter by X-Ray Single Crystal Diffraction and Calculations B3LYP/6-31G* Levels for Complex 2

	Exptl.	B3LYP/6-31G*
Bond lengths (Å)		
Ir(1)—Ir(2)	2.715(6)	2.6203
N(4)-N(5)	1.106(7)	1.1168
Ir(2)—N(4)	1.927(7)	2.0338
Ir(2)—C(31)	2.095(5)	2.0390
Ir(1)—N(1)	2.060(4)	2.0807
Ir(1)—N(3)	2.024(4)	2.0689
Ir(2)—N(2)	2.138(5)	2.2190
Ir(1)—C(1)	2.000(5)	2.0038
Ir(2)—C(16)	2.045(6)	2.0202
Ir(1)—C(45)	1.985(5)	2.0904
Bond Angle (deg)		
N(5)- N(4)-Ir(2)	172.1(7)	172.65
N(4)-Ir(2)-Ir(1)	96.9(9)	94.01
N(4)-Ir(2)-C(31)	175.3(2)	178.08
N(1)-Ir(1)-C(1)	79.81(19)	80.58
N(3)-Ir(1)-N(1)	173.2(1)	177.85
Dihedral Angle (deg)		
N(3)- Ir(1)- Ir(2)- N(4)	167.4(2)	163.11

(6) Table S2. Calculated Absorption of Complex 2 in CH₂Cl₂ Media at TD-B3LYP Level, Together with Experimental Values

States	$\lambda(\text{nm}) / E(\text{eV})$	oscillator	main configurations	assign	Exptl.
S ₁	716.17 / 1.73	0.0170	H→L (99.49%)	Ir1/Ir2/pq→Ir1/pq (MLCT/LLCT)	
S ₁₇	407.74 / 3.04	0.0222	H→L+6 (35.49%)	Ir1/Ir2/pq→Ir1/Ir2/pq (LLCT/MLCT/ILCT)	385
S ₁₈	402.79 / 3.08	0.0267	H→L+5 (85.95%)	Ir1/Ir2/pq→pq (MLCT/LLCT/ILCT)	385
S ₂₈	360.10 / 3.44	0.1449	H-6→L (37.06%)	Ir1/Ir2/pq→Ir2/pq (MLCT/LLCT)	346
S ₅₀	318.99 / 3.89	0.0626	H-8→L+1 (56.47%)	Ir1/Ir2/pq→Ir2/pq (MLCT/LLCT/ILCT)	

(6) Table S3. The photophysical properties of complex 2^a

Complex	2
Absorption	242, 278,
wavelength	346, 385
$\lambda(\text{nm})$	
Solution luminescence	582
$\lambda(\text{nm})$	
Φ_{PL}	0.025

^a Absorption and emission spectra were recorded in spectroscopic grade dichloromethane at 298 K. Quantum yields of emission were measured in degassed dichloromethane solutions, using Alq₃ in DMF ($\Phi_{\text{PL}}=0.116$) as a reference.

(6) Table S4. The UV-vis absorption wavelength of complex 2 and pq

Complex	2	pq
Absorption wavelength $\lambda(\text{nm})$	242, 278, 346, 385	225, 258, 322.50